Relationship between energetic disorder and open-circuit voltage in bulk heterojunction organic solar cells

James C. Blakesley* and Dieter Neher
Department of Physics and Astronomy, University of Potsdam, Potsdam, Germany
(Received 8 April 2011; revised manuscript received 13 May 2011; published 12 August 2011)

We simulate organic bulk heterojunction solar cells. The effects of energetic disorder are incorporated through a Gaussian or exponential model of density of states. Analytical models of open-circuit voltage (V_{OC}) are derived from the splitting of quasi-Fermi potentials. Their predictions are backed up by more complex numerical device simulations including effects such as carrier-density–dependent charge-carrier mobilities. It is predicted that the V_{OC} depends on: (1) the donor-acceptor energy gap; (2) charge-carrier recombination rates; (3) illumination intensity; (4) the contact work functions (if not in the pinning regime); and (5) the amount of energetic disorder. A large degree of energetic disorder, or a high density of traps, is found to cause significant reductions in V_{OC}. This can explain why V_{OC} is often less than expected in real devices. Energetic disorder also explains the nonideal temperature and intensity dependence of V_{OC} and the superbimolecular recombination rates observed in many real bulk heterojunction solar cells.

DOI: 10.1103/PhysRevB.84.075210 PACS number(s): 88.40.jr

I. INTRODUCTION

With internal quantum efficiencies approaching 100%,[1] there are two approaches to further enhancing the power efficiency of bulk heterojunction organic photovoltaics (BHJ OPVs). The first is to improve the matching between the absorption of the solar cell and the solar spectrum by using narrow-band-gap donor materials, alternative acceptor components, or by building tandem solar cells. The second approach is to increase the open-circuit voltage (V_{OC}) without loss of photocurrent. Unfortunately, our understanding of the way in which V_{OC} is determined is quite incomplete, and it is not clear how devices can be engineered to increase V_{OC} without a loss of quantum efficiency.

Many studies have shown that V_{OC} depends on the energy gap between the highest occupied molecular orbital (HOMO) level of the donor component and the lowest unoccupied molecular orbital (LUMO) level of the acceptor component of the BHJ.[2–4] Perhaps the most famous of these is the work of Scharber *et al.*,[2] which studied V_{OC} across a wide range of materials combinations. They found an empirical relationship: $eV_{OC} = E_g - 0.3\,eV$, where E_g is the donor-acceptor energy gap, and e is the elementary charge. While this study was invaluable to engineering a new generation of donor polymers, it gives little physical insight as to the origins of V_{OC}. The question has often been asked: What causes the 0.3 eV loss, and how can it be reduced?

As V_{OC} denotes the voltage at which the total current is zero, it depends fundamentally on the balance between charge-carrier generation and recombination in the active region. Recent studies have found that a reliable forecast of V_{OC} can be achieved by measuring charge-carrier recombination rates under open-circuit conditions.[5,6] They have also been able to account for the dependence of V_{OC} on light intensity by considering the variation in carrier density with voltage.

Intriguingly, several studies[7–9] have found strong correlations between the energy of emissive charge-transfer (CT) states and V_{OC}. This observation raises the question of whether its dependence on the donor-acceptor energy gap is causal, or just coincidental. Using the principles of detailed balance, it was argued that the CT state energy would determine V_{OC} if radiative CT state decay is the limiting loss mechanism.[10] It has been suggested that reducing CT state emission might be a route to improving device performance, though many uncertainties remain, such as the effects of nonradiative losses.[11]

In recent years, it has become clear that the energetic structure of solid films of conjugated materials is complex, and the reduction of a model to simple, well-defined, energy levels is an oversimplification. For example, inhomogeneous broadening of HOMO or LUMO energy levels (energetic disorder) is typically thought to lead to a spread of states across an energy range of 0.1 eV or more. When charge carriers are photogenerated, they will inevitably relax within this distribution of states, leading to a loss of energy. In devices, this could be reflected in a drop in V_{OC}. A couple of recent publications have predicted such behavior in a Gaussian density of states (DOS).[12,13] In this paper, we expand on this work using both Gaussian and exponential DOS distributions with analytical and numerical models. In the first section, an analytical model for V_{OC} in a system with energetic disorder is derived. Next, we introduce a numerical device simulation including realistic physical phenomena, such as contact mirror-charge potentials, field-assisted dissociation, and density-dependent charge-carrier mobilities. Finally, we compare the results of the numerical simulations to the predictions of the analytical model.

II. ANALYTICAL MODEL

In a BHJ solar cell, the rate of recombination of charge carriers is dependent on the carrier density. A higher carrier density results in a higher recombination rate. In turn, the carrier density of a device depends on the voltage. As voltage is increased into forward bias, the internal field due to the built-in voltage is reduced, and the carrier density increases. In the most general approach to predicting V_{OC}, V_{OC} is the voltage at which the recombination rate exactly matches the photogeneration rate. This was demonstrated neatly by Maurano

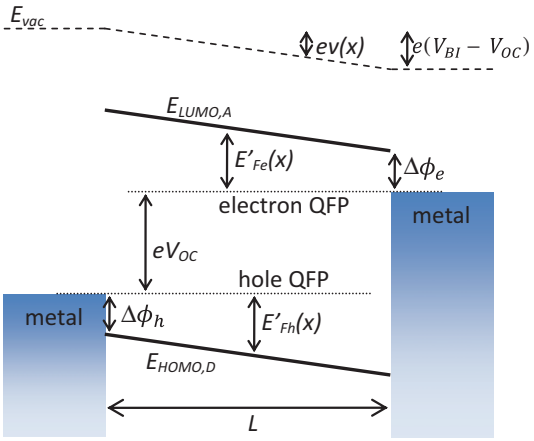

FIG. 1. (Color online) Energy-level diagram showing an OPV device at open-circuit voltage. E_{vac} is the vacuum level, and all other symbols are as defined in the text. All energy intervals are defined as positive as shown in this diagram.

et al.,[6] who measured recombination rates and carrier densities under open-circuit conditions at different light intensities. Recombination rates were parameterized by an empirical power-law dependence on carrier density, while carrier density was parameterized by an empirical exponential dependence on voltage. When combined, these gave a logarithmic dependence of V_{OC} upon light intensity, in agreement with experiments. While this general approach is able to describe the behavior of many different material systems, it is thoroughly empirical and gives little physical insight into the origins of differences between materials. In contrast, the ideal BHJ diode model derived by Koster[14] represents a specific case of this general behavior. It predicts V_{OC} in terms of physical parameters, such as the donor-acceptor energy gap and recombination rate coefficient. While insightful, this model fails to predict the precise dependence of V_{OC} on light intensity for the majority of real devices. In this section, we begin by deriving once again V_{OC} for an ideal device. We then demonstrate that, by including the effects of energetic disorder, we are able to reproduce the more general, nonideal, behavior observed in real devices.

Note that V_{OC} in real devices is also affected by external device properties, such as series and shunt resistances. These can particularly complicate the accurate measurement of true cell V_{OC}. In this paper, we focus on the fundamental physical limits of V_{OC}, and such external issues are ignored.

We start by deriving V_{OC} for a system without disorder by considering Fermi-level splitting. Consider the energy-level diagram in Fig. 1, which shows a BHJ device at V_{OC}. The device consists of an active layer sandwiched between two metallic electrodes. The active layer represents the donor-acceptor blend. It is treated as an effective medium in which the electron transport level is defined by the LUMO of the acceptor material, while the hole transport level is defined by the HOMO of the donor material.

We apply a constant electron-hole pair generation rate, G, throughout the active region. At V_{OC}, the generation of charge carriers must be exactly balanced by charge-carrier recombination; otherwise a net current would result. If all carriers recombine close to where they are generated when the device is at V_{OC}, then the local recombination rate, $R(x)$, is equal to the local generation rate:

$$R(x) = G, \tag{1}$$

where x is the depth within the active region. At V_{OC}, no net current flows by definition. It follows that electron and hole currents must both be zero, and the quasi-Fermi potentials (QFPs) for electrons and holes will therefore be constant and aligned with the Fermi levels of the electron- and hole-injecting contacts, respectively. The electron and hole QFPs will be separated by eV_{OC}. We can then write the hole and electron quasi-Fermi potentials relative to their respective energy levels as (see Fig. 1):

$$E'_{Fh}(x) = \Delta\phi_h + ev(x) \tag{2}$$

and

$$E'_{Fe}(x) = \Delta\phi_e - ev(x) - eV_{OC} + eV_{BI}, \tag{3}$$

where $v(x)$ is the local internal electrical potential due to external voltage, built-in voltage, V_{BI}, and space-charge, and $\Delta\phi_h$ and $\Delta\phi_e$ are the hole and electron injection barriers, respectively. V_{BI} is defined here as the difference in the contact work functions. For the moment, we treat the hole and electron energy levels as narrow bands and apply the Boltzmann approximation to obtain the respective local carrier densities for holes and electrons:

$$n_h(x) = N_h \exp\left[\frac{-\Delta\phi_h - ev(x)}{k_B T}\right] \tag{4}$$

and

$$n_e(x) = N_e \exp\left[\frac{-\Delta\phi_e + ev(x) + eV_{OC} - eV_{BI}}{k_B T}\right] \tag{5}$$

where N_h and N_e are the total density of states for holes and electrons (in the donor-acceptor blend), respectively, k_B is Boltzmann's constant, and T is temperature. The rate of charge-carrier recombination is critical to the determination of V_{OC}, though the physics underlying it are not fully understood. One fact that is well established is that recombination rates depend on the densities of both charge carriers. To begin with, we assume that direct bimolecular recombination is the dominant form of recombination. In this case, the recombination rate can be written as:

$$R(x) = \gamma n_h(x) n_e(x), \tag{6}$$

where γ is the recombination rate coefficient. The Langevin formula,[15] $\gamma_L = e(\mu_h + \mu_e)/\varepsilon\varepsilon_0$, where μ_h and μ_e are the electron and hole mobility, provides an upper limit of recombination coefficient, giving the rate at which electrons and holes encounter one another. While the Langevin rate assumes diffusion in a homogeneous medium, the rate has been confirmed as reasonable in fine-scale donor-acceptor blends by Monte Carlo simulations[16] as long as electron and hole mobilities are reasonably balanced. These simulations assumed that carriers have a 100% chance of recombination when they encounter each other. In the case that the decay rate of the Coulombically bound electron-hole pair is low enough that carriers can diffuse apart from each other again before recombining, the recombination rate might be significantly lower than that predicted by Langevin. Indeed, studies using a

variety of different techniques have found that recombination rates are often far below this limit.[5,17]

We can combine Eqs. (1), (4), (5), and (6) to get a familiar expression for the open-circuit voltage:[14]

$$eV_{\mathrm{OC}} = E_g + k_B T Ln\left(\frac{G}{\gamma N_h N_e}\right), \tag{7}$$

where E_g $(= \Delta\phi_h + \Delta\phi_e + eV_{BI} = E_{\mathrm{HOMO},D} - E_{\mathrm{LUMO},A})$ is the effective energy gap for the donor-acceptor blend. This formula predicts many of the features of previous experimental observations, such as the direct dependence of V_{OC} on donor-acceptor energy gap[2–4] and recombination rate.[5,6] Using typical values for generation and recombination rates, one finds that the second term above is in the region of -0.2 to -0.5 eV at solar intensity. According to this model, the 0.3 eV loss in the Scharber[2] scheme can be explained by the balance between recombination and generation, while the large scatter in V_{OC} for different materials can be explained by material-dependent variations in recombination rates. However, as will be discussed later, this is not the complete story. Most real devices do not follow the intensity dependence predicted by the ideal model, and variation in the densities of states should also be considered.

According to the principles of thermodynamics, the charge pair generation rate, G, must be the sum of an optical component, G_{opt}, which is proportional to the incident photon flux, and a thermal-generation component, G_{therm}. By detailed balance, the latter must equal the recombination rate when at thermal equilibrium in the dark, giving:

$$G_{\mathrm{therm}} = \gamma N_h N_e \exp\left(-\frac{E_g}{k_B T}\right). \tag{8}$$

Substituting $G = G_{\mathrm{opt}} + G_{\mathrm{therm}}$ into Eq. (7), we get:

$$eV_{\mathrm{OC}} = E_g + k_B T Ln\left[\exp\left(-\frac{E_g}{k_B T}\right)\left(1 + \frac{G_{\mathrm{opt}}}{G_{\mathrm{therm}}}\right)\right]. \tag{9}$$

The thermal and optical generation rates can be measured from the reverse-bias saturation dark current density, $J_0 = eLG_{\mathrm{therm}}$, and reverse-bias saturation photocurrent density, $J_{\mathrm{ph}} = eLG_{\mathrm{opt}}$, respectively. In the case that recombination at short circuit is negligible, the latter equates to the short-circuit current, J_{SC}. We then find

$$V_{\mathrm{OC}} = \frac{mk_B T}{e} Ln\left(\frac{J_{\mathrm{SC}}}{J_0} + 1\right), \tag{10}$$

where $m = 1$ is the ideality factor. This is the same result as the famous Shockley equation for *p-n* junction devices,[18] despite the fact that here we are modeling BHJ devices. This relationship between dark current and open-circuit voltage has been demonstrated experimentally in bilayer OPVs.[19,20] Vandewal *et al.*[8] found that good predictions of V_{OC} in BHJs were made when J_0 was derived by detailed balance from electroluminescence and photocurrent quantum efficiencies instead of dark current. Experimentally, the ideality factor, m, is nearly always found to be greater than 1 in OPVs.[8,21,22] Previously, we assumed direct bimolecular recombination and found $m = 1$ in Eq. (10). If, instead, we write recombination as a power-law in carrier density, n, in Eq. (6): $R \propto n^{\alpha}$, then the ideality factor becomes $m = 2/\alpha$. In inorganic *p-n* junction diodes, $m = 2$ is found at low voltages, and $m = 1$ is found at higher voltage.[23] The behavior is attributed to indirect recombination by the trapping of minority carriers, which is a monomolecular recombination process. OPVs have heterojunctions instead of *p-n* junctions, and there are no minority carriers, though it is conceivable that a similar recombination process could occur by trapping of carriers at a heterojunction interface. However, experimental studies of recombination in BHJ OPVs consistently show that recombination is bimolecular, or even *super*-bimolecular at higher intensities.[24–26] This is inconsistent with an ideality factor greater than 1 according to the previous analysis. Later herein, we suggest that energetic disorder can explain this discrepancy.

The electronic states of molecules in an organic semiconductor film are subject to random energetic variations as a result of factors such as variations in conjugation length, rotations and kinking of polymer chains, interactions with neighboring conjugated molecules, impurities and dipoles from residual solvent molecules, etc. Note that this disorder is not intrinsic to the molecular structure, but it is a property of the solid film. It is strongly dependent on film preparation. The result of this energetic disorder is that the bands in the DOS corresponding to the HOMO and LUMO states do not have well-defined onsets. Instead, a tail of low-energy states extends far into the nominal energy gap (see Fig. 2). Experimental evidence for such tail states is strong. Several recent experiments have measured their energetic distribution sensitively in various materials.[24,27–30] They found that tails could be approximated to Gaussian or exponential distributions with typical widths of the order of 0.1 to 0.2 eV. Other studies have used energetic disorder to explain various phenomena in organic semiconductors, such as temperature-, field-, and carrier density–dependent charge-carrier mobility,[31–34] reduced charge injection barriers,[35] and increased band bending at interfaces.[36,37] Intrinsic dopant levels are typically very low in organic semiconductors, such that the tail states are not completely filled in OLED and OPV operation. The relaxation of carriers into deep tail states then must be considered as an important process in determining device performance.

We now derive the expression for V_{OC} Eq. (7) for devices with energetic disorder. To simulate the effect of a broadly distributed DOS onset, we use two different model DOS distributions: (a) Gaussian distribution and (b) exponential distribution. We write the model DOS as:

$$g_{h/e}(E) = \frac{N_{h/e}}{\sigma\sqrt{2\pi}} \exp\left[-\frac{(\pm E \mp E_{\mathrm{HOMO},D/\mathrm{LUMO},A})^2}{2\sigma^2}\right], \tag{11a}$$

$$g_{h/e}(E) = \frac{N_{t,h/e}}{E_t} \exp\left[\pm\frac{E - E_{\mathrm{HOMO},D/\mathrm{LUMO},A}}{E_t}\right], \tag{11b}$$

respectively, where E is energy, $E_{\mathrm{HOMO},D}$ and $E_{\mathrm{LUMO,A}}$ are representative of the donor HOMO energy level and acceptor LUMO energy level, σ quantifies the energetic disorder in the Gaussian distribution, and E_t is the characteristic energy for the exponential tail distribution. Care should be taken about the use of "HOMO" or "LUMO" to describe energy levels. Their use to refer to the frontier orbitals of a single isolated

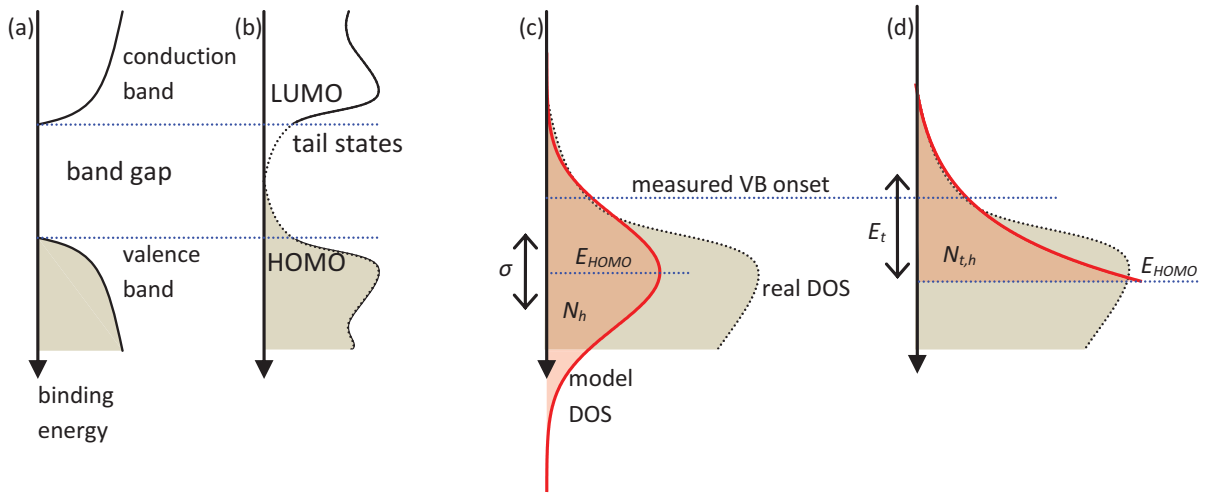

FIG. 2. (Color online) Schematic density of states (DOS) for (a) classical crystalline inorganic semiconductor and (b) disordered organic semiconductor showing tail states extending into the band gap. (c) and (d) A Gaussian or exponential DOS respectively (red lines) used to approximate the tail of the valence states. The widths of the model DOS are σ and E_t, and the areas enclosed are N_h and $N_{t,h}$, respectively.

molecule is clear, but their meaning in the context of a realistic disordered solid film where localized and delocalized states may exist together is not well defined. Often, in practice, the terms are used to refer to onset of valence or conduction states measured experimentally by techniques such as photoemission spectroscopy or cyclic voltammetry. These might be better described as valence band (VB) and conduction band (CB) onsets. Since these onsets are determined by the energy at which the states first become visible relative to the background signal, the measured values are subject to the sensitivity of the experimental method and instrumental broadening. While a Gaussian or exponential model might not accurately represent the entire DOS of a real solid, the majority of occupied states are within the tail of the distribution, below the measured onset. In choosing a model DOS, we aim only to describe the shape of the tail-states distribution. $E_{\mathrm{HOMO},D}$ and $E_{\mathrm{LUMO},A}$ are mathematical terms. Typically, the measured VB and CB onsets are offset from $E_{\mathrm{HOMO},D}$ or $E_{\mathrm{LUMO},A}$ in the direction of the energy gap by up to 3 times σ or E_t [see Figs. 2(c) and 2(d)].[29,36,37]

The carrier density is calculated by integrating the Fermi-Dirac distribution across the DOS. For the Gaussian distribution at low[38] carrier densities, this can be approximated by a Boltzmann distribution[13]

$$n_h(x) = N_h \exp\left[\frac{\sigma^2}{2(k_BT)^2}\right] \exp\left[\frac{-E'_{Fh}(x)}{k_BT}\right]. \quad (12a)$$

for holes, where E'_{Fh} is the difference between the hole quasi-Fermi potential and $E_{\mathrm{HOMO},D}$, and the same applies for electrons. Substituting in place of Eqs. (4) and (5), we arrive at a similar result for the open-circuit voltage:

$$eV_{\mathrm{OC}} = E_g^{\mathrm{eff}} + k_BT\,Ln\left(\frac{G}{\gamma N_h N_e}\right), \quad (7a)$$

where E_g is replaced by the new effective donor-acceptor energy gap, $E_g^{\mathrm{eff}} = E_{\mathrm{HOMO},D} - E_{\mathrm{LUMO},A} - \sigma^2/k_BT$. We find that a broader DOS causes a lower effective energy gap, and therefore a lower V_{OC}. This can be understood intuitively as a loss of energy as charge carriers relax within the DOS until they occupy low-energy sites, thus bringing the average energy of positive and negative charge carriers closer together.

For the exponential distribution, if $E_t \gg k_BT$, then the carrier density for holes can be approximated by:

$$n_h(x) = N_{t,h} \exp\left[\frac{-E'_{Fh}(x)}{E_t}\right]. \quad (12b)$$

and the equivalent for electrons. Now the V_{OC} becomes:

$$eV_{\mathrm{OC}} = E_g + mk_BT\,Ln\left(\frac{G}{\gamma N_{t,h} N_{t,e}}\right), \quad (7b)$$

where $E_g = E_{\mathrm{HOMO},D} - E_{\mathrm{LUMO},A}$, and $m = E_t/k_BT$. The k_BT in Eq. (7) is replaced by mk_BT, which again leads to loss of V_{OC}. This substitution can also be made for Eqs. (8), (9), and (10). Equation (7a) predicts ideal diode behavior for a Gaussian DOS, while Eq. (7b) predicts nonideal behavior for an exponential DOS. In both cases, eV_{OC} maintains its one-to-one dependence on the donor-acceptor energy gap, though the tail states are responsible for an additional loss.

III. NUMERICAL MODEL

In deriving an analytical model for V_{OC}, it is necessary to simplify many aspects of the device physics. Using a drift-diffusion device model that incorporates a Gaussian or exponential density of states, we are able to test the robustness of the results in more realistic physical conditions. In our model, we include the effects of surface recombination at the electrodes, field-dependent geminate-pair separation, and carrier-density–dependent charge-carrier mobilities. To simplify matters, we assume that acceptor electron and donor

hole mobilities, densities of states, and disorder are identical throughout.

The model uses the standard drift-diffusion form to calculate the current density for both holes and electrons:

$$J = -e\mu n\frac{dv}{dx} \pm eD\frac{dn}{dx}, \tag{13}$$

where J is current density, n is carrier density, μ is mobility, and D is the diffusion coefficient. This is solved simultaneously with the one-dimensional Poisson's equation:

$$\frac{d^2v}{dx^2} = \frac{e\left(n_e - n_h\right)}{\varepsilon\varepsilon_0}, \tag{14}$$

where ε_0 is the permittivity of free space, and ε is the relative permittivity, under the boundary condition that the voltage dropped across the active region is equal to the applied voltage minus the difference in electrode work functions.

There is currently a debate as to whether free-carrier generation in BHJ OPVs is electric field dependent or not. It certainly seems to depend on the material in question. There is clear evidence of field-dependent carrier generation in some single-component OPVs and all-polymer BHJ devices.[39,40] To take account of this, we used the approach of Koster *et al.*[41] It is assumed that all photogenerated electron-hole pairs are generated in an initially Coulombically bound state (polaron pairs or geminate pairs). These bound pairs can either dissociate into free carriers with probability $p(x)$, or decay to the ground state. Similarly, bimolecular recombination involves the coming together of free electrons and holes to form bound pairs at rate of $R(x)$. A fraction, $p(x)$, of these will dissociate back into free carriers again without decaying to the ground state. The probability of dissociation depends on the binding energy and decay rate of the bound state, temperature, electric field, the free-carrier mobility, and the structure of the donor/acceptor interface in a BHJ. To simplify this, we use the approach of Braun.[42] In this model, a field-dependent dissociation rate competes with a field-independent decay rate. Here, we write the explicit field and mobility dependence of dissociation, while the all other parameters are summarized by a single material-dependent constant, β (see note [43] for an explanation of β):

$$p(x) = \frac{\beta(\mu_h + \mu_e)}{\beta(\mu_h + \mu_e) + \sqrt{-2b}/J_1(2\sqrt{-2b})} \tag{15}$$

where J_1 is the first-order Bessel function, $b = e^3F\left(x\right)/8\pi\varepsilon\varepsilon_0k_B^2T^2$, and $F(x)$ is the electric field. This is only a rough approximation of true dissociation—simulations have shown that disorder complicates matters[44] and that a broad distribution of binding energies should be considered.[45] We use direct bimolecular recombination rates according to Langevin to estimate the rate at which electrons encounter holes, $R\left(x\right) = \gamma_L n_e n_h$,[15] with $\gamma_L = e\left(\mu_h + \mu_e\right)/\varepsilon\varepsilon_0$. Note that an increase in mobility reduces the probability of geminate recombination without disturbing the equilibrium between free carriers and bound carriers, since carriers will also encounter each other at a faster rate.

Finally, the current continuity equation under steady-state conditions is applied for electrons and holes:[41]

$$\frac{dJ}{dx} + \left[1 - p\left(x\right)\right]R\left(x\right) - p\left(x\right)G = 0 \tag{16}$$

To include the effects of bound-pair dissociation in the analytical model presented earlier, we note that the equilibrium condition is now $pG = (1 - p)\,R$.[14] Making the assumption that the field is close to zero in open-circuit conditions, we find that Eqs. (7), (7a), (7b), and (7c) (below) can be approximated by using a reduced recombination coefficient, $\gamma = \gamma_L/\beta\left(\mu_h + \mu_e\right)$. Studies of bimolecular recombination rates in blends of poly(3-hexyl-thiophene) (P3HT) with a fullerene derivative have revealed values of the order of 10^{-1} to 10^{-3} of the Langevin rate.[5,17,26] Similar factors have been observed in some other materials,[46] though it is not yet clear whether this behavior is general to all efficient BHJ materials. These reduced recombination rates could be caused by charge carriers coming into contact with each other but not recombining. Such materials also happen to be ones in which field-dependent dissociation is not an important mechanism,[47,48] indicating that the bound-pair decay rate is low, that the bound-state binding energy is small, or that free-carrier mobilities are high, and hence bound pairs are most likely dissociated again before they have a chance to decay to the ground state.[11] In these cases, values for $\beta\left(\mu_h + \mu_e\right)$ of order 100 are appropriate to model the suppression of Langevin recombination. For comparison, simulations were also performed using the conventional non-field-dependent continuity equation: $dJ/dx + R - G = 0$, using Langevin recombination rates. To include the effects of energetic disorder, we need to consider two factors. Firstly, the Boltzmann approximation does not always apply for the carrier density as a function of Fermi potential. The diffusion constant, D, in Eq. (13) must be calculated as a function of carrier density according to the generalized Einstein relation.[49] Secondly, in a system with energetic disorder, it has been established[33] that mobility increases with charge-carrier density as a result of the filling up of the lowest energy states. The exact manner in which the mobility varies depends on the model used. Here, we compare two models: the Gaussian disorder model (GDM)[31] and the mobility edge (ME) (also called multiple trapping and retrapping) model.[50] Both models have been successfully used to model charge transport in disordered materials,[32,34,51,52] and both predict an increase in charge-carrier mobility with increasing charge-carrier densities. The former is applied to a Gaussian density of states, as in Eq. (11a), and assumes that all sites are highly localized, with charge transport occurring by hopping between these localized states. The carrier-density dependence of mobility for the GDM has been calculated using various methods.[53–55] Here, we use a variant of the parameterization scheme of Pasveer[53] to calculate the mobility for each carrier type as a function of x:

$$\mu\left(x\right) = \mu_0 \exp\left\{-0.42\hat{\sigma}^2 + \frac{1}{2}(\hat{\sigma}^2 - \hat{\sigma})\left[2n\left(x\right)/N\right]^{\delta}\right\}$$
$$\delta = 2\frac{ln(\hat{\sigma}^2 - \hat{\sigma}) - 0.3266}{\hat{\sigma}^2}, \tag{17a}$$

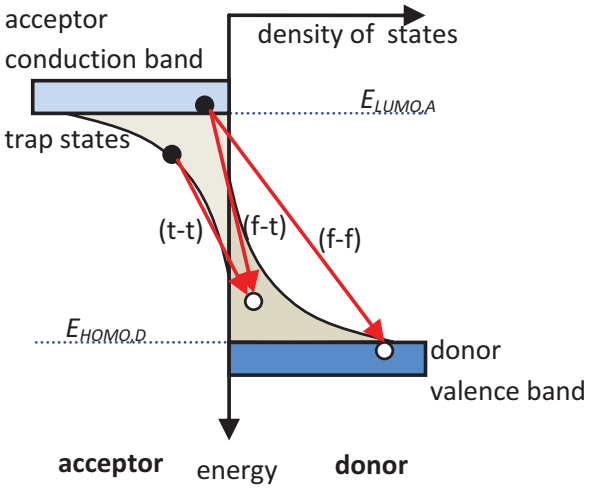

FIG. 3. (Color online) Schematic diagram illustrating different recombination modes in mobility-edge model. (t-t) trapped-carrier to trapped-carrier recombination; (f-t) free-carrier to trapped-carrier recombination; and (f-f) free-carrier to free-carrier recombination.

where μ_0 is the high-temperature limit of mobility, $\hat{\sigma} = \sigma/k_BT$ is the amount of disorder relative to thermal energy, and N is the total density of states.

For the mobility edge model, it is assumed that there exists a dense band of delocalized states with effective density N at energy $E_{\mathrm{HOMO},D}$ or $E_{\mathrm{LUMO},A}$, through which charge transport occurs with mobility μ_0. An exponential tail of trap states extends from the band into the band gap with distribution as given in Eq. (11b). Assuming that no charge transport can occur between trap states, the effective mobility is given by:[50]

$$\mu(x) = \mu_0 \frac{n_f}{n_f + n_t}, \tag{17b}$$

where n_f is the density of free carriers in the delocalized band, and n_t is the density of carriers in the trap states. Under the assumption that trapping and detrapping are sufficiently rapid, thermal equilibrium is established between these two populations. They are determined by the relative position of the quasi-Fermi potential, E_F':

$$\begin{aligned} n_f &= N \exp\left(-\frac{E_F'}{k_BT}\right), \\ n_t &\approx N_t \exp\left(-\frac{E_F'}{E_t}\right), \\ n &= n_f + n_t. \end{aligned} \tag{18}$$

There are three possibilities for modeling recombination in the mobility-edge model (see Fig. 3): (1) Recombination can only occur between free electrons and free holes (f-f). In this case, the trap distribution plays no role in determining V_{OC}, and Eq. (7) remains unchanged. (2) Bimolecular recombination can occur between free carriers and trapped charge (f-t). In BHJ devices, this process differs fundamentally from Shockley-Read-Hall recombination, since electrons and holes do not coexist in the same material component. Instead, it can be considered that free carriers in one component are attracted to the trapped charge in the other component. If the trapped charge is sufficiently close to a heterojunction interface, then the mutual attraction could cause it to detrap and recombine with the free carrier. In this case, we apply a bimolecular recombination rate following the Langevin form $R = e\mu_0(n_e n_{h,f} + n_h n_{e,f})/\varepsilon\varepsilon_0$. (3) Carriers trapped in the tail states are allowed to recombine directly with other trapped carriers (t-t). We model this using a bimolecular recombination rate, $R = 2e\mu_0 n_e n_h/\varepsilon\varepsilon_0$. While the third case is theoretically interesting, it seems physically unlikely that t-t recombination would contribute significantly to the recombination current in a real device. We study both cases 2 and 3 here, though case 2 should be considered the most realistic model.

Notice that n_f increases superlinearly with n. Considering case 2, this leads to an apparent increase in the bimolecular recombination rate at higher carrier densities. Such a phenomenon might explain the various observations of recombination rates with power-law density dependencies greater than 2.[24–26] If $n_t \gg n_f$, as might be the case under typical OPV operating conditions, the process is dominated by recombination between free carriers and trapped carriers. Assuming hole and electron densities are equal, this gives a power-law behavior $R \propto n^\alpha$ with $\alpha \approx 1 + (E_t/k_BT)$. In this situation, we need to revise Eq. (7b) in order to predict V_{OC}, giving:

$$\begin{aligned} eV_{\mathrm{OC}} &= E_g + mk_BT\,Ln\left(\frac{G}{\gamma N_t N}\right), \\ m &= \frac{2}{1 + k_BT/E_t}, \\ \gamma &= e\mu_0/\varepsilon\varepsilon_0. \end{aligned} \tag{7c}$$

For the following numerical simulations, devices of thickness $L = 100$ nm were simulated by dividing them into at least 400 equally spaced grid points. For both disorder models, the following parameters were used: mobility $\mu_0 = 10^{-3}$ cm^2/Vs, density of states $N = 10^{21}$ cm^{-3}, donor-acceptor energy gap $E_g = 2$ eV, relative permittivity $\varepsilon = 3.5$, and a dissociation parameter $\beta = 5 \times 10^4$ Vs/cm^2. All simulations were performed at $T = 300$ K. Boundary conditions for the numerical simulation were that the electron and hole quasi-Fermi potentials in the first and last grid points were aligned with the contact Fermi levels, i.e., $E_F'(0) = \Delta\phi_h$, $E_F'(L) = \Delta\phi_e$. Studies of injection currents[35,56–58] have demonstrated that the reduction of injection barriers by a mirror-charge potential is an important effect when injection barriers are large. To account for this, an additional term, $\Delta v(x)$ was added to the electron potential and subtracted from the hole potential:

$$\Delta v(x) = \frac{e}{16\pi\varepsilon\varepsilon_0}\left(\frac{1}{x} + \frac{1}{L-x}\right). \tag{19}$$

When the injection barrier is small, the mirror-charge potential can be ignored due to screening from the large carrier density at the contact. However, when the injection barriers are large, it creates an additional surface recombination current that can significantly affect open-circuit voltage, as reported in the results section. The simulation also reproduces well the high- and low-field injection currents predicted by Emtage and O'Dwyer[56] in the absence of energetic disorder.

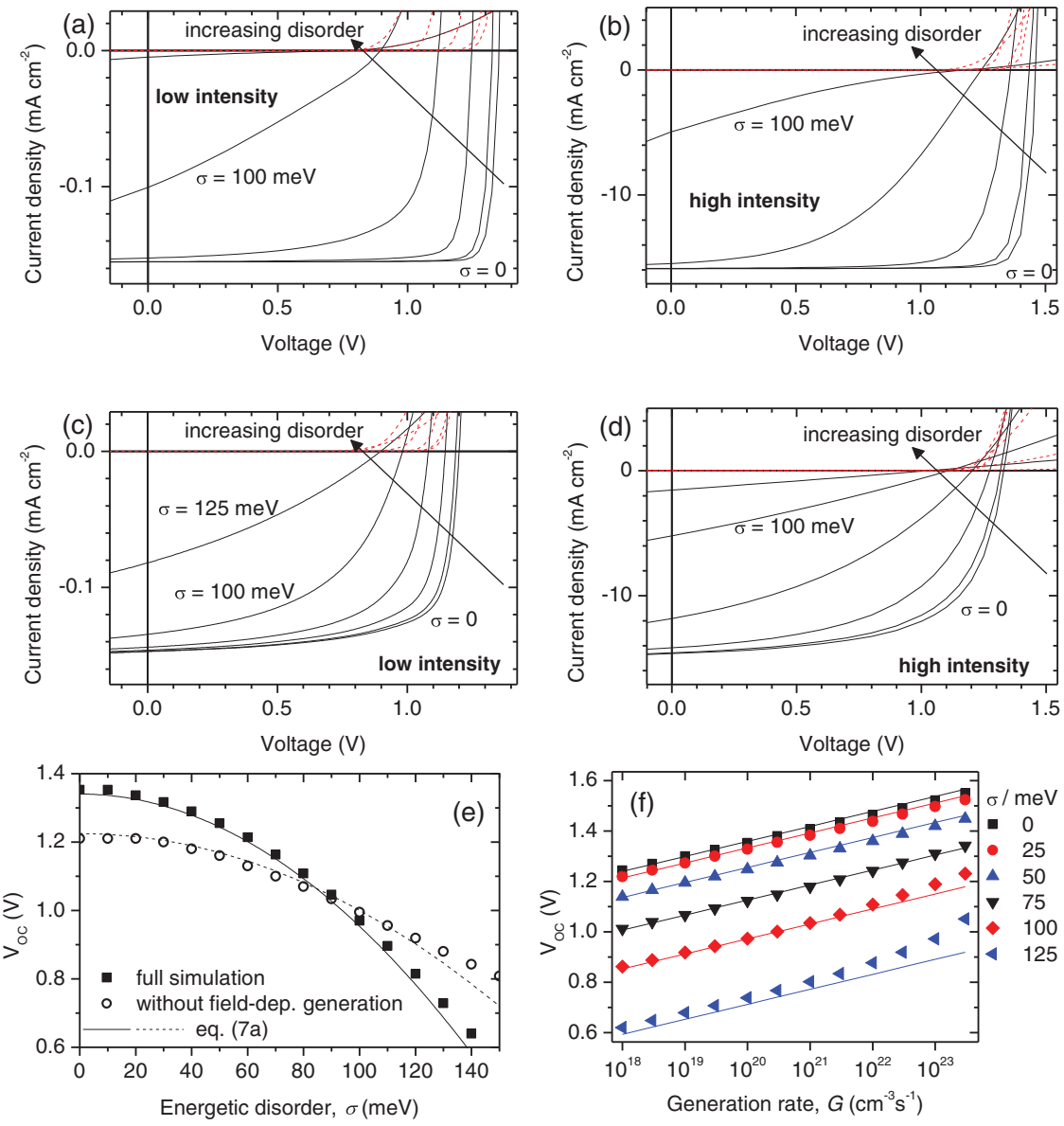

FIG. 4. (Color online) Simulations of BHJ devices with Gaussian disorder. (a) and (b) Simulated current-voltage curves for varying degrees of disorder ($\sigma = 0$, 25, 50, 75, 100, and 125 meV) at low ($G = 10^{20}$ cm^{-3}s^{-1}) and high ($G = 10^{22}$ cm^{-3}s^{-1}) intensities, respectively. (Dashed red lines are dark currents.) (c) and (d) Same as (a) and (b) except without field-dependent generation and recombination rates. (e) V_{OC} vs. disorder at low intensity. Filled symbols: using field-dependent continuity equation [Eq. (16)]. Open symbols: using field-independent continuity equation. Solid line: Eq. (7a) with effective recombination coefficient $\boldsymbol{\gamma} = \boldsymbol{\gamma}_L/\boldsymbol{\beta}(\boldsymbol{\mu}_h + \boldsymbol{\mu}_e)$. Dashed line: Eq. (7a) with $\boldsymbol{\gamma} = \boldsymbol{\gamma}_L$. (f) V_{OC} vs. intensity with varying disorder and field-dependent generation and recombination. Symbols: numerical simulation; solid lines: Eq. (7a).

IV. RESULTS

First, we consider devices with Ohmic contacts, where there is no injection barrier for electrons or holes. Figure 4 shows the results of numerical simulations of devices using the GDM with varying degrees of disorder. Figures 4(a) and 4(b) shows simulated current-voltage curves for devices at low and high intensities, respectively. The latter ($G = 10^{22}$ cm^{-3}s^{-1}) is comparable to 1 sun intensity in typical OPVs. Without disorder, a very high fill factor is observed. As disorder is increased, the fill factor drops dramatically, and the simulation starts to resemble more realistic devices. The drop in fill factor is attributable to the drop in mobility with increasing disorder. This occurs through two mechanisms. Firstly, dissociation of bound electron-hole pairs becomes less efficient, leading to large geminate losses at low electric fields. Secondly, bimolecular recombination losses become more predominant as charge-carrier extraction becomes slower. This is especially true at high intensities.[59,60] For comparison, Figs. 4(c) and 4(d) shows the same curves for simulations in which the field dependence of free-carrier generation and recombination was neglected. The impact of disorder is stronger in Figs. 4(a) and 4(b) as low disorder results in a reduced recombination rate, while high disorder results in a strongly field-dependent generation rate.

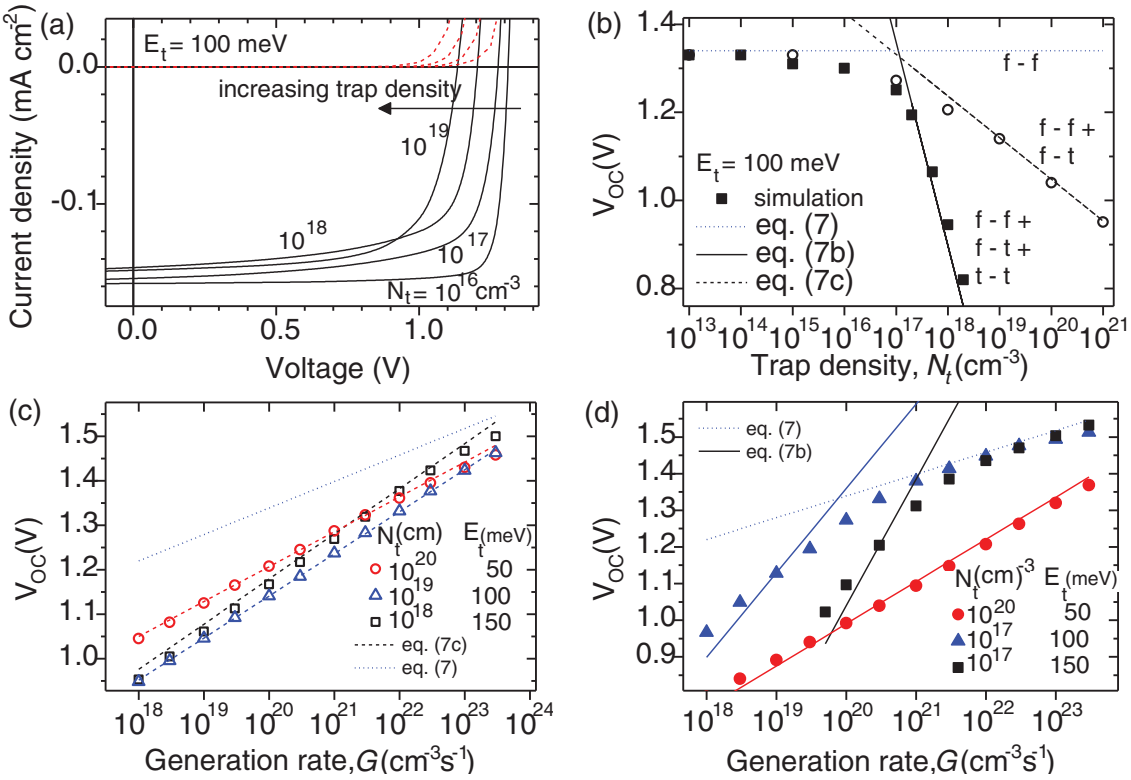

FIG. 5. (Color online) Simulations of BHJ devices with exponential density of trap states. (a) Simulated current-voltage curves with E_t = 100 meV and varying trap densities ($N_t = 10^{16}$, 10^{17}, 10^{18}, and 10^{19} cm^{-3}) at low ($G = 10^{20}$ cm^{-3}s^{-1}) intensity. (b) V_{OC} vs. trap density for the same conditions. Filled symbols: including trap-to-trap recombination (t-t); open symbols: excluding trapped-to-trapped recombination, but including free-to-trapped-carrier recombination (f-t). (c) V_{OC} vs. intensity excluding trapped-to-trapped recombination for different trap distributions. (d) V_{OC} vs. intensity including trapped-to-trapped recombination for different trap distributions. Lines: analytical solutions from text.

Concurrent with the decline in fill factor, a large decrease in V_{OC} is seen as disorder is increased. Figure 4(e) plots V_{OC} as a function of disorder at low intensity, and Fig. 4(f) shows the dependence of V_{OC} on intensity for varying disorder. Also shown are the V_{OC} values predicted from Eq. (7a). This predicts well the results of the simulations at low intensities. At high intensities, and large quantities of disorder, the simulated V_{OC} starts to grow more quickly with intensity than predicted by the ideal diode equation, and Eq. (7a) no longer applies. Instead, it is necessary to include an ideality factor to fit the predictions, despite the fact that recombination is still strictly bimolecular. The nonideality arises from the failure of the Boltzmann approximation in Eq. (12a)—the real carrier density varies more rapidly with the Fermi potential than predicted there.

Figure 5 shows the results of simulations using the ME model with exponential density of trap states. Simulations were performed both with and without the inclusion of recombination of trapped electrons with trapped holes (t-t). In both cases, recombination was allowed between trapped electrons and free holes and vice versa (f-t). Figure 5(a) shows the simulated current-voltage characteristics as the density of trap states is varied at low intensities without (t-t) recombination. Once again, both the fill factor and V_{OC} fall as the density of trap states is increased. The decline in fill factor is not as dramatic as that noted previously since the free-carrier mobility remains unchanged in this case, and therefore bound-pair dissociation is not affected by the presence of traps in this model. One should be careful not to pay too much attention to the simulated fill factors, however, because the effect of disorder and trapping on the field dependence of pair dissociation is still quite debatable.[44,45] Figure 5(b) shows the variation of V_{OC} with trap density at low intensity, while Figs. 5(c) and 5(d) shows the variation of V_{OC} with intensity for different trap distributions. When (t-t) recombination is allowed, V_{OC} is predicted reasonably well by Eq. (7b) at low intensities and high trap densities. When (t-t) recombination is excluded, Eq. (7c) predicts V_{OC}. In both cases, in the limit of high intensity or low trap density, we reach a point at which the traps become completely filled, and the carriers become blind to the presence of traps. In this case, V_{OC} is limited by the properties of band-like transport only, and the behavior is as predicted by Eq. (7) for ideal diodes without disorder. Therefore, according to the ME model, there is a critical trap density, below which V_{OC} is not reduced. For 1 sun intensity and assuming E_t = 100 meV, this limit is of the order of 10^{17} to 10^{18} cm^{-3}.

Figure 6 shows energy-level diagrams for devices simulated under open-circuit conditions with and without Gaussian disorder. It is interesting to note that the electric field in the middle of the device is almost the same in both cases, despite the voltage being reduced by a factor by about 0.8 V when disorder is included. The additional internal voltage is almost entirely taken up by an increase in band bending near to the contact interfaces. Recently, such band bending was observed in Kelvin-probe studies at various metal/conjugated

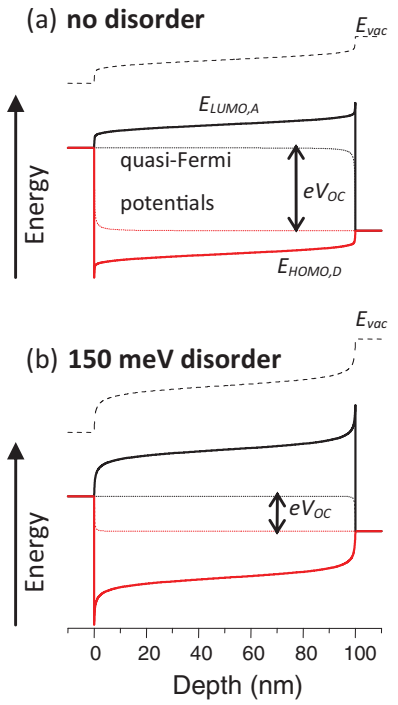

FIG. 6. (Color online) Simulated energy diagrams in open-circuit conditions with $G = 10^{20}$ cm^{-3}s^{-1} and (a) no disorder. (b) $\sigma =$ 150 meV Gaussian disorder.

polymer interfaces.[37] The magnitude of the band bending was consistent with predictions of models including a significant amount of energetic disorder. More disorder causes more band bending, and it was noted[13] that the predicted loss of V_{OC} due to Gaussian disorder is equal in magnitude to the increase in band bending. It has been suggested that band bending directly causes a loss of V_{OC}.[4,61,62] However, such a causal link is difficult to demonstrate, especially since there is no need to explicitly include band bending in the derivation of Eq. (7a). At least it is possible to state that increased band bending is concomitant with a loss of V_{OC}. For this reason, we advocate further experimental investigations into the link between band bending and V_{OC}.

In a simple metal-insulator-metal (MIM) model of a BHJ device, V_{OC} cannot exceed the built-in voltage of the contacts. Biasing beyond the built-in voltage will reverse the internal electric field and therefore also the direction of the photocurrent. This limit does not apply to bilayer solar cells,[63] where reverse photocurrents are blocked.

Experiments on poly(phenylene-vinylene) (PPV) derivatives blended with different acceptor molecules[4,64] found that eV_{OC} had a one-to-one dependence on cathode work function when the electron injection barrier was large. However, when the cathode work function was small enough to make an Ohmic contact to the acceptor component, V_{OC} became independent of cathode work function, but instead had a one-to-one dependence on the acceptor reduction potential. In other words, V_{OC} can be limited either by the effective donor-acceptor energy gap, or by the difference in contact work functions. In the analytical model derived earlier, it was assumed that the contacts were completely selective (each quasi-Fermi potential was aligned to one contact only), and the effects of surface recombination currents were ignored. This leads to the elimination of contact work functions from the model. In reality, there will be an additional loss mechanism besides bimolecular recombination as some carriers leave the device by drift and/or diffusion to the contacts. In open-circuit conditions, these additional "surface" recombination currents must be equal for electrons and holes at each contact in order to maintain steady-state charge densities in the contacts. Therefore, if either polarity of charge carrier is blocked from reaching a contact, then this loss vanishes. With Ohmic contacts, a large carrier density is present near the electrode interface (as verified by our own recent experiments [37]). This charge causes carriers of the opposite polarity to recombine before reaching the contact. They are also repelled by the strong band bending present near the interface. The agreement between the analytical model and the numerical simulations confirms that surface recombination losses are negligible under normal conditions. The concept that surface recombination is negligible for Ohmic contacts has been demonstrated theoretically,[65] while recent experiments have shown that nonbimolecular losses are negligible at V_{OC} in P3HT:methanofullerene solar cells.[66] By simulating devices

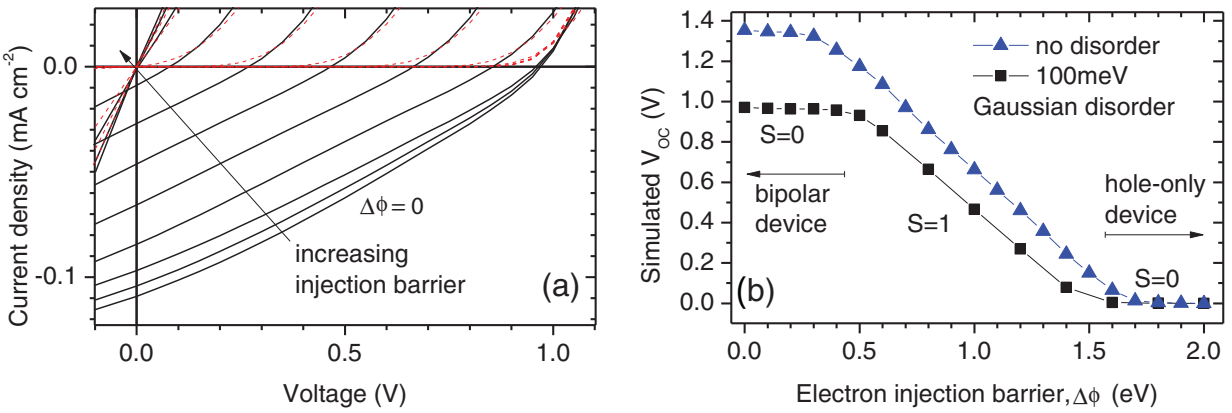

FIG. 7. (Color online) Simulations of BHJ devices with Gaussian disorder and varying electron injection barriers. (a) Current-voltage characteristics for devices with $\sigma = 100$ meV and $G = 10^{20}$ cm^{-3}s^{-1}. (b) V_{OC} vs. electron injection barrier under the same conditions with and without disorder.

of different thicknesses (not shown), we found that V_{OC} begins to decline significantly as the thickness is reduced below about 20 nm. When the image potential [Eq. (19)] was omitted from the simulations, V_{OC} remained independent of device thickness. This indicates that surface recombination driven by recombination between carriers and their own mirror charge can become significant in devices with Ohmic contacts only when the device thickness is of the order of the Coulomb capture radius ($r_C = e^2/4\pi\varepsilon\varepsilon_0 k_B T$) or less.

If a significant injection barrier is present at one of the contacts, then there is expected to be a significant surface recombination current as photogenerated electrons and holes flow toward the contact in an attempt to establish an equilibrium with the contact Fermi level, while the blocking effect discussed previously is removed. This reduces V_{OC}. Naturally, a homogeneous device with two identical contacts should have no V_{OC} at all. This was tested by running simulations of devices with varying electron injection barriers for the low work-function contact. The resulting current-voltage characteristics for devices with 100 meV Gaussian disorder are shown in Fig. 7(a). For small injection barriers, changes in contact work function have little effect. When the injection barrier becomes larger than about 0.4 eV, the whole current-voltage characteristic shifts to lower voltages, and the V_{OC} is reduced.

Figure 7(b) shows V_{OC} as a function of the electron injection barrier. Interestingly, a z-curve emerges that is reminiscent of the Fermi-level pinning behavior observed in photoemission spectroscopy and Kelvin studies[36,37,67] of conjugated materials deposited on substrates with different work functions. When the contact Fermi level lies close to either $E_{HOMO,D}$ or $E_{LUMO,A}$, V_{OC} is independent of the contact work function. Between these limits, there is a slope of 1. This is quite consistent with experimental observations.[4,64] As previously observed, disorder reduces V_{OC} when both contacts are Ohmic. Notice, that the effect of disorder is exactly halved when only one of the contacts is pinned. It was shown recently[37] that the limits of Fermi-level pinning in polymer films of more than about 10 nm thickness were governed by band bending. Again, these results are suggestive of a strong correlation between band bending and V_{OC}. However, the simple MIM model in which the V_{OC} is equal to the built-in voltage minus the amount of band bending at each contact is not quite right. V_{OC} depends on intensity, while band bending does not; similarly, band bending depends on the thickness of the active layer, while V_{OC}, in principle, does not.

V. DISCUSSION

The core principle of this paper is that energetic disorder will reduce V_{OC}. Interestingly, this result has also been predicted for a Guassian DOS using quite different methods.[12] It has also long been known that tail states in amorphous silicon cause a reduction in V_{OC} by trapping minority carriers, leading to an increase in recombination.[68] Together, these findings demonstrate the robustness of the principle, despite the different theoretical approaches.

This paper has focused on theoretical aspects of open-circuit voltage. When attempting to apply such theories to experimental results, we are faced with the problem of not knowing precisely the DOS of the materials that we are studying. Take, for example, researchers' favorite material system of poly(3-hexyl-thiophene) (P3HT) blended with [6,6]-phenyl C_{61} butyric acid methyl ester (PCBM). The difference between the onset of oxidation in P3HT and the onset of reduction in PCBM has been measured at about 0.8 eV,[2] while others find that the energy gap between donor and acceptor HOMO/LUMO onsets is more like 1.1 eV.[24] In order to apply Eq. (7a) to predict V_{OC}, we need to make many assumptions about the DOS where information is not available. The energetic disorder in P3HT is quite small, estimated about $\sigma = 70$ meV,[69] and we can assume a similar magnitude for PCBM. As mentioned previously, the appropriate position for the center of the model DOS could be up to 3σ beyond the measured onset of valence/conduction states. Therefore, an appropriate $E_{HOMO,D} - E_{LUMO,A}$ could be ~1.2 eV, and the effective energy gap with disorder accounted for will be $E_g^{\text{eff}} \approx$ 1.0 eV. We have to make another assumption about the total density of states for electrons and holes. Here, we will assume 10^{21} cm^{-3} for each. Transient measurements of recombination give typical values of the order of $\gamma = 10^{-12}$ m^{3}s^{-1},[5,47,70] though these vary greatly depending on material preparation. Finally, taking $G = 10^{22}$ cm^{-3}s^{-1} for 1 sun intensity, Eq. (7a) gives us $V_{OC} \approx 0.55$ V. While this estimate agrees well with typical measured values, the vast number of assumptions about the DOS leads to uncertainties of at least ± 0.2 V. It is clear that more detailed studies of the DOS of donor-acceptor blends are necessary to make advances in this area.

Our results also suggest that disorder is a possible origin of the nonideal diode behavior found in most BHJ OPVs. An intensity-dependent transition from ideal to nonideal behavior is predicted. One of the notable differences between the GDM and ME models is that the GDM predicts ideal behavior at low intensities and nonideal behavior at high intensities, while the opposite is the case for the ME model. Experimentally, this transition is not usually observed, though the range of intensities that can be studied can be quite limited due parasitic series and shunt resistances. It remains difficult to choose between the models, and some transport studies even combine them both.[71] In both models, the nonideality coincides with a dependence of mobility on carrier density. This can explain observations of apparent power-law dependence of recombination rate on intensity,[5,17,24–26] though these could also result from voltage-dependent nonuniform charge distributions.[72] While physically different from Shockley-Read-Hall (SRH) recombination in homojunction devices, the (f-t) recombination process treated in this paper can be regarded as a specific class of SRH recombination with distributions of trap states close to the valence band maximum and conduction band minimum that are neutral when empty (i.e., nondoping), and that have Langevin capture cross-sections when occupied. A very recent publication used this approach and arrived independently at the same nonideal behavior in dark currents.[73] Care should be taken not to overextend this analogy with SRH: It is still unclear how heterojunction morphology interacts with (f-t) recombination.

Several reports have suggested a strong correlation between the energy of emissive charge transfer (CT) states and V_{OC}.[7–9,11] It was found that measurements of CT state emission and absorption energy were more strongly correlated to V_{OC} than measurements of donor/acceptor oxidation/reduction potentials. There are two possible explanations. Firstly, the

relationship could be coincidental. CT states can be thought of as hybrid excitons formed between the donor HOMO and acceptor LUMO states. The CT state energy is therefore strongly related to the donor-acceptor energy gap, and it might be a more reliable predictor of the effective energy gap than independent measurements of donor/acceptor valence/conduction state onsets by other techniques. It is not surprising to find a correlation between CT state energy and V_{OC}, even if the CT state plays only a minor role in device performance.

The second explanation is that there is a causal relationship between CT state energy and V_{OC}. Consider the case that charge-carrier recombination is mediated through the decay of radiative CT states. If CT state decay is the primary pathway to recombination, *and* CT state decay is slow enough, then CT states will dissociate into free carriers faster than they can decay. This will be manifest in a reduced effective recombination rate, which will lead in turn to an increase in V_{OC}. In this case, the recombination rate will be $R_{CT} = n_{CT}/\tau_{CT}$, where n_{CT} is the density of excited CT states, and τ_{CT} is the CT state lifetime. As charge carriers repeatedly encounter each other and separate again, the occupancy of CT states will be in balance with the number of free carriers. Therefore, the probability of a CT state being occupied will depend on the applied voltage and the energy of the CT state. Under these specific conditions, V_{OC} depends not only on the CT state energy, but also the lifetime, density, and energetic distribution of CT states. To some extent, the CT state energy is already included via the Braun treatment of bound-pair dissociation,[11] though there is confusion over the definition of a CT state. In the context of the Braun model, it refers to a Coulombically bound pair of mobile charge carriers that can have a range of the order of 10 nm. In the context of spectroscopy, it refers to a highly localized emissive interfacial excitation.

Vandewal *et al.*[10] showed by detailed balance that efficient OPVs should also make efficient electroluminescent devices, because suppression of nonradiative recombination will lead to a higher V_{OC} and quantum efficiency. The highest electroluminescent quantum efficiency of the OPVs they measured was of the order of 0.0001%, demonstrating that the vast majority of bimolecular recombination is nonradiative. It is not clear whether spectroscopy of radiative CT states alone gives much insight into the dominant recombination pathways. The CT-limited recombination hypothesis also fails to explain so far the super-bimolecular recombination behavior. While this hypothesis should not be ruled out, further experiments are required.

VI. CONCLUSIONS

Numerical device simulations including field-dependent bound-pair dissociation, mirror charge potentials, and two different models of energetic disorder were performed. The results demonstrated that energetic disorder can be responsible for a loss of open-circuit voltage in BHJ OPVs. The results of the numerical simulations can be described by a simple analytical expression in many, but not all, cases. We found that energetic disorder can also account for the nonideal diode behavior and intensity-dependent recombination rates often observed in real OPVs.

While the link between V_{OC} and energetic disorder is not yet proven, there is a strong incentive for the community to improve methods of quantifying the distribution of tail states, and to study their impact on device performance. Tackling the effects of energetic disorder could be a key to improving OPV efficiency beyond 10%.

ACKNOWLEDGMENTS

J.C.B. would like to thank Neil Greenham of the University of Cambridge for interesting discussions that fomented this work.

*james.blakesley@physics.org

[1] S. H. Park, A. Roy, S. Beaupré, S. Cho, N. Coates, J. S. Moon, D. Moses, M. Leclerc, K. Less, and A. J. Heeger, Nat. Photonics **3**, 297 (2009).

[2] M. C. Scharber, D. Mühlbacher, M. Koppe, P. Denk, C. Waldauf, A. J. Heeger, and C. J. Brabec, Adv. Mater. **18**, 789 (2006).

[3] T. Kietzke, D. A. M. Egbe, H.-H. Hörhold, and D. Neher, Macromolecules **39**, 4018 (2006).

[4] V. D. Mihailetchi, P. W. M. Blom, J. C. Hummelen, and M. T. Rispens, J. Appl. Phys. **94**, 6849 (2001).

[5] C. G. Shuttle, B. O'Regan, A. M. Ballantyne, J. Nelson, D. D. C. Bradley, and J. R. Durrant, Phys. Rev. B **78**, 113201 (2008).

[6] A. Maurano, R. Hamilton, C. G. Shuttle, A. M. Ballantyne, J. Nelson, B. O'Regan, W. Zhang, I. McCulloch, H. Azimi, M. Morana, C. J. Brabec and J. R. Durrant, Adv. Mater. **22**, 4987 (2010).

[7] K. Vandewal, A. Gadisa, W. D. Oosterbaan, S. Bertho, F. Banishoeib, I. V. Severen, L. Lutsen, T. J. Cleij, D. Vanderzande, and J. V. Manca, Adv. Funct. Mater. **18**, 2064 (2008).

[8] D. Veldman, S. C. J. Meskers, and R. A. J. Janssen, Adv. Funct. Mater. **19**, 1939 (2009).

[9] K. Tvingstedt, K. Vandewal, A. Gadisa, F. Zhang, J. Manca, and O. Ingenäs, J. Amer. Chem. Soc. **131**, 11819 (2009).

[10] K. Vandewal, K. Tvingstedt, A. Gadisa, J. V. Manca, Nat. Mater. **8**, 904 (2009).

[11] C. Deibel, T. Strobel, V. Dyakonov, Adv. Mater. **22**, 4097 (2010).

[12] G. Garcia-Belmonte and J. Bisquert, Appl. Phys. Lett. **96**, 113301 (2010).

[13] J. C. Blakesley and N. C. Greenham, J. Appl. Phys. **106**, 034507 (2009).

[14] L. J. A. Koster, V. D. Mihailetchi, R. Ramaker, and P. W. M. Blom, Appl. Phys. Lett. **86**, 123509 (2005).

[15] P. Langevin, Ann. Chim. Phys. **7**, 433 (1903).

[16] C. Groves and N. C. Greenham, Phys. Rev. B **78**, 155205 (2008).

[17] M. P. Eng, P. R. F. Barnes, and J. R. Durrant, J. Phys. Chem. Lett. **1**, 3096 (2010).

[18] P. Würfel, *Physics of Solar Cells*, 2nd ed. (Wiley-VCH, New York, 2009).

[19] W. J. Potscavage Jr., A. Sharma, and B. Kippelen, Acc. Chem. Res. **42**, 1758 (2009).

[20] M. D. Perez, C. Borek, S. R. Forrest, and M. E. Thompson, J. Amer. Chem. Soc. **131**, 9281 (2009).

[21]B. P. Rand, D. P. Burk, and S. R. Forrest, Phys. Rev. B **75**, 115327 (2007).
[22]C. Waldauf, M. C. Scharber, P. Schilinsky, J. A. Hauch, and C. J. Bravec, J. Appl. Phys. **99**, 104503 (2006).
[23]S. M. Sze, *Semiconductor Devices*, 2nd ed. (John Wiley & Sons, New York, 2002).
[24]G. Garcia-Belmonte, P. P. Boix, J. Bisquert, M. Sessolo, and H. J. Bolink, Sol. Ener. Mater. and Sol. Cells **94**, 366 (2010).
[25]G. Juska, K. Genevicius, N. Nekrasas, G. Sliauzys, and G. Dennler, Appl. Phys. Lett. **93**, 143303 (2008).
[26]C. G. Shuttle, B. O'Regan, A. M. Ballantyne, J. Nelson, D. D. C. Bradley, J. de Mello, and J. R. Durrant, Appl. Phys. Lett. **92**, 093311 (2008).
[27]T. Sueyoshi, H. Fukagawa, M. Ono, S. Kera, and N. Ueno, Appl. Phys. Lett. **95**, 183303 (2009).
[28]O. Tal, Y. Rosenwaks, Y. Preezant, N. Tessler, C. K. Chan, and A. Kahn, Phys. Rev. Lett. **95**, 256405 (2005).
[29]I. N. Hulea, H. B. Brom, A. J. Houtepen, D. Vanmaekelbergh, J. J. Kelly, and E. A. Meulenkamp, Phys. Rev. Lett. **93**, 166601 (2004).
[30]K. Celebi, P. J. Jadhav, K. M. Milaninia, M. Bora, and M. A. Baldo, Appl. Phys. Lett. **93**, 083308 (2008).
[31]H. Bässler, Phys. Stat. Sol. B **175**, 15 (1993).
[32]S. L. M. van Mensfoort and R. Coehoorn, Phys. Rev. B **78**, 085207 (2008).
[33]C Tanase, E. J. Meijer, P. W. M. Blom, and D. M. de Leeuw, Phys. Rev. Lett. **91**, 216601 (2004).
[34]J. C. Blakesley, H. S. Clubb, and N. C. Greenham, Phys. Rev. B **81**, 045210 (2010).
[35]V. I. Arkhipov, E. V. Emelianova, Y. H. Tak, and H. Bässler, J. Appl. Phys. **84**, 848 (1998).
[36]J. Hwang, A. Wan, and A. Kahn, Mater. Sci. and Eng. **R64**, 1 (2009).
[37]I. Lange, J. C. Blakesley, J. Frisch, A. Vollmer, N. Koch, and D. Neher, Phys. Rev. Lett. **106**, 216402 (2011).
[38]This approximation is valid as long as the Fermi potential is more than σ^2/k_BT below the center of the distribution, corresponding to $n_{n/e} < N_{h/e}\ \exp[-(3\sigma/2k_BT)^2]$.
[39]M. Esteghamatian, Z. D. Popovic, and G. Xu, J. Phys. Chem. **100**, 13716 (1996).
[40]R. A. Marsh, C. R. McNeil, A. Abrusci, A. R. Campbell, and R. H. Friend, Nano Lett. **8**, 1393 (2008).
[41]L. J. A. Koster, E. C. P. Smits, V. D. Mihailetchi, and P. W. M. Blom, Phys. Rev. B **72**, 085205 (2005).
[42]C. L. Braun, J. Chem. Phys. **80**, 4157 (1980).
[43]In terms of Ref. 42, we can write $\beta = eK(0)/k_f\varepsilon\varepsilon_0$, where k_f is the bound-pair decay rate, and $K(0)$ is the equilibrium constant for dissociation at zero field, which depends on the relative energy and entropy of bound and free states. Two possible forms for $K(0)$ are given in Ref. 42, though it is debatable whether either is applicable to the case of a BHJ interface. The equilibrium constant depends on the ratio of the number of possible free- and bound-state configurations available within the system, which will depend on factors such as the donor-acceptor interfacial area and the quantum-mechanical nature of the bound states. Neither of these is considered in the Braun model.
[44]C. Groves, R. A. Marsh, and N. C. Greenham, J. Chem. Phys. **129**, 114903 (2008).
[45]C. Groves, J. C. Blakesley, and N. C. Greenham, Nano Lett. **10**, 1 (2010).
[46]M. J. Tan, W.-P. Goh, J. Li, G. Pundir, V. Chellappan, and Z.-K. Chen, Appl. Mater. Interf. **2**, 1414 (2010).
[47]J. Kniepert, M. Schubert, J. C. Blakesley and D. Neher, J. Phys. Chem. Lett. **2**, 700 (2011).
[48]R. Mauer, I. A. Howard, and F. Laquai, J. Phys. Chem. Lett. **1**, 3500 (2010).
[49]Y. Roichman and N. Tessler, Appl. Phys. Lett. **80**, 1948 (2002).
[50]P. Mark and W. Helfrich, J. Appl. Phys. **33**, 205 (1962).
[51]R. Steyrleuthner, S. Bange and D. Neher, J. Appl. Phys. **105**, 064509 (2009).
[52]A. Salleo, T. W. Chen, A. R. Völkel, Y. Wu, P. Liu, B. S. Ong, and R. A. Street, Phys. Rev. B **70**, 115311 (2004).
[53]W. F. Pasveer, J. Cottaar, C. Tanase, R. Coehoorn, P. W. M. Blom, D. M. de Leeuw, and M. A. J. Michels, Phys. Rev. Lett. **94**, 206601 (2005).
[54]I. I. Fishchuk, V. I. Arkhipov, A. Kadashchuk, P. Heremans, and H. Bässler, Phys. Rev. B **76**, 045210 (2007).
[55]L. Li, S. Van Winckel, J. Genoe, and P. Heremans, Appl. Phys. Lett. **95**, 153301 (2009).
[56]P. R. Emtage and J. J. O'Dwyer, Phys. Rev. Lett. **16**, 356 (1966).
[57]J. C. Scott and G. G. Malliaras, Chem. Phys. Lett. **299**, 115 (1999).
[58]Z. B. Wang, M. G. Helander, M. T. Greiner, J. Qiu, and Z. H. Lu, Phys. Rev. B **80**, 235325 (2009).
[59]P. W. M. Blom, V. D. Mihailetchi, L. J. A. Koster, and D. E. Markov, Adv. Mater **19**, 1551 (2007).
[60]M. Lenes, M. Morana, C. J. Brabec, and P. W. M. Blom, Adv. Funct. Mater. **19**, 1106 (2009).
[61]M. Kemerink, J. M. Kramer, H. H. P. Gommans, and R. A. J. Janssen, Appl. Phys. Lett. **88**, 192108 (2006).
[62]P. Kumar, S. C. Jain, H. Kumar, S. Chand, and V. Kumar, Appl. Phys. Lett. **94**, 183505 (2009).
[63]D. Cheyns, J. Poortmans, P. Heremans, C. Deibel, S. Verlaak, B. P. Rand, and J. Genoe, Phys. Rev. B **77**, 165332 (2008).
[64]C. J. Brabec, A. Cravino, D. Meissner, N. S. Sariciftci, T. Fromherz, M. T. Rispens, L. Sanchez, and J. C. Hummeln, Adv. Funct. Mater. **11**, 374 (2001).
[65]H. Bässler, Polym. Adv. Technol. **9**, 402 (1998).
[66]C. G. Shuttle, A. Maurano, R. Hamilton, B. O'Regan, J. C. de Mello, and J. R. Durrant, Appl. Phys. Lett. **93**, 183501 (2008).
[67]S. Braun, W. R. Salaneck, and M Fahlman, Adv. Mater. **21**, 1450 (2009).
[68]T. Tiedje, Appl. Phys. Lett. **40**, 627 (1982).
[69]A. J. Mozer and N. S. Sariciftci, Chem. Phys. Lett. **389**, 438 (2004).
[70]J. M. Guo, H. Ohkita, H. Benten, and S. Ito, J. Am. Chem. Soc. **132**, 6154 (2010).
[71]Y. Zhang, B. de Boer, and P. W. M. Blom, Phys. Rev. B **91**, 085201 (2010).
[72]C. Deibel, A. Wagenpfal, and V. Dyakonov, Phys. Rev. B **80**, 075203 (2009).
[73]T. Kirchartz, B. E. Pieters, J. Kirkpatrick, U. Rau, and J. Nelson, Phys. Rev. B **83**, 115209 (2011).